Topography of vision and behaviour

Jochen Smolka* and Jan M. Hemmi

ARC Centre of Excellence in Vision Science, Centre for Visual Sciences, Research School of Biology, The Australian National University, Canberra ACT 2601, Australia

*Author for correspondence (jochen.smolka@anu.edu.au)

SUMMARY

Given the great range of visual systems, tasks and habitats, there is surprisingly little experimental evidence of how visual limitations affect behavioural strategies under natural conditions. Analysing this relationship will require an experimental system that allows for the synchronous measurement of visual cues and visually guided behaviour. The first step in quantifying visual cues from an animal's perspective is to understand the filter properties of its visual system. We examined the first stage of visual processing – sampling by the ommatidial array – in the compound eye of the fiddler crab *Uca vomeris*. Using an *in vivo* pseudopupil method we determined sizes and viewing directions of ommatidia and created a complete eye map of optical and sampling resolution across the visual field. Our results reveal five distinct eye regions (ventral, dorsal, frontal, lateral and medial) which exhibit clear differences in the organisation of the local sampling array, in particular with respect to the balance of resolution and contrast sensitivity. We argue that, under global eye space constraints, these regional optimisations reflect the information content and behavioural relevance of the corresponding parts of the visual field. In demonstrating the tight link between visual sampling, visual cues and behavioural strategies, our analysis highlights how the study of natural behaviour and natural stimuli is essential to our understanding and interpretation of the evolution and ecology of animal behaviour and the design of sensory systems.

INTRODUCTION

All animals rely on sensory information to guide their behaviour. However, sensory systems are limited in the amount and quality of information they can provide. To understand an animal's behaviour, we therefore have to understand the limitations of its sensory systems. Conversely, the design of sensory systems in many cases reflects the distribution of behaviourally relevant information an animal is confronted with under natural conditions (e.g. Gibson, 1950; Loew and Lythgoe, 1985; Lythgoe and Partridge, 1989; Simoncelli and Olshausen, 2001; Körding et al., 2004) and the organisation of an animal's behaviour (e.g. Srinivasan, 1993; Eckert and Zeil, 2001; Sparks, 2005). In addition, both sensory systems and behavioural strategies are constrained by an animal's phylogeny, development and physiology. Eyes and visual systems, in particular, are energetically costly (Niven and Laughlin, 2008), leading to a wide variety of global (e.g. Krapp and Hengstenberg, 1996) and regional (Walls, 1942; Hughes, 1977; Land, 1989) eye specialisations that serve to extract specific and relevant information. These specialisations exploit the fact that biologically relevant information is not randomly distributed in visual space. Similar events tend to happen in similar regions of the observer's visual field, whether this is through ecological and topological constraints or through active movements of eyes, head and body. Examples of regional eye specialisations are abundant in both vertebrates and invertebrates: regionalisations of acuity and sensitivity, such as in the fovea of many vertebrates (Walls, 1942; Hughes, 1977) and in the visual streak of flat-world inhabitants like fiddler crabs (Zeil et al., 1986; Land and Layne, 1995a; Zeil and Al-Mutairi, 1996), specialisations for target tracking in predatory and mate-chasing insects (for review, see Land, 1989), or regionalisations of the

spectral (e.g. Arikawa, 2003; Marshall et al., 2007), polarisation (e.g. Labhart, 1980; Dacke et al., 2003; Marshall et al., 2007) or temporal sensitivities (e.g. Burton et al., 2001) of photoreceptors. However, considering this diversity of adaptations, there is very limited evidence of how the global design of eyes and the distribution of different regional specialisations reflect the informational ecology of animals and affect their behavioural strategies. For three main reasons, fiddler crabs (genus *Uca*) present a unique opportunity to investigate this question.

Firstly, the crabs' small home-range, burrow-centred lifestyle and the organisation of their visual system allow us to simultaneously monitor the complete behaviour and the flow of behaviourally relevant information available to individual crabs (Zeil and Hemmi, 2006). Their compound eyes are situated on long stalks which are kept perpendicular to the visual horizon at all times (Nalbach et al., 1989; Zeil and Al-Mutairi, 1996). Each eye has a panoramic visual field, making it unnecessary for the animal to perform any directed or scanning eye movements. This makes it possible to reconstruct the complete visual information available to an individual crab at any one time and map it onto the compound eyes simply by monitoring an animal's position and orientation.

Secondly, fiddler crabs rely almost exclusively on vision in a wide variety of behavioural tasks including predator avoidance (Land and Layne, 1995a; Land and Layne, 1995b; Hemmi, 2005a; Hemmi, 2005b), homing (Zeil, 1998; Layne et al., 2003a; Layne et al., 2003b), territory defence (e.g. Altevogt and von Hagen, 1964; von Hagen, 1967; Land and Layne, 1995a; Land and Layne, 1995b; Hemmi and Zeil, 2003a; Hemmi and Zeil, 2003b), mate choice (Detto et al., 2006) and courtship signalling (How et al., 2007; How and Hemmi, 2008). These behaviours are limited in different ways

by the capabilities and accuracy of the visual system (e.g. Land and Layne, 1995b; Hemmi, 2005a; Hemmi, 2005b; Hemmi and Zeil, 2005). In some *Uca* species, for example, individual recognition is based on the coloured patterns on the crabs' carapaces (Detto et al., 2006; Detto et al., 2008). Distinguishing these patterns requires high visual acuity and good colour vision. Predator avoidance, on the other hand, does not require the formation of a coloured or high-resolution image at all, but rather relies on high sensitivity in individual receptors to detect a small object as early as possible.

Thirdly, in compound eyes there is a direct trade-off between the number of ommatidia looking into a certain visual angle (which determines sampling resolution, i.e. the 'pixelation' of the image) and the size of individual ommatidial lenses [which determines the receptive field size, local contrast sensitivity and optical resolution, i.e. the blurring of the image due to diffraction in the lens (Land, 1981; Warrant and McIntyre, 1993)]. Regionalisation of these parameters can be evaluated using non-invasive optical techniques: facet diameters can be directly measured from micrographs, and the viewing directions of individual ommatidia are indicated by the pseudopupil, a black spot that marks the ommatidia that look directly into the observing optics' aperture and follows the observer around the eye (Franceschini, 1975; Stavenga, 1979).

In this study, we used *in vivo* optical techniques to create the first complete eye map for a fiddler crab compound eye. We examined the regional specialisations of resolving power and contrast sensitivity in the eyes of *Uca vomeris* and relate them to behaviour, social signals and colour vision. By carefully measuring the movements of the pseudopupil as a camera was rotated in known angular steps around the eye, we determined the visual axes of ommatidia – and thus sampling resolution – and the diameter of facet lenses – and thus optical resolution – over almost the entire *U. vomeris* compound eye. Our results show clear differences in the organisation of the sampling array between five eye regions (ventral, dorsal, frontal, lateral and medial). These local specialisations are closely associated with different aspects of the crabs' behaviour. We argue that these regions are specialised to support different behavioural tasks and that, in turn, the organisation of the crabs' behaviour supports and enables these structural differences.

MATERIALS AND METHODS
Animals, morphology and optical apparatus

Fiddler crabs *Uca vomeris* McNeill (Ocypodidae: Brachyura: Decapoda) of both sexes and of a wide range of sizes (10–25 mm carapace width, measured between lateral carapace spines) were collected from intertidal mudflats near Cungulla (19°24′S, 147°6′E), south of Townsville, Queensland, Australia and Redland Bay (27°37′S, 153°17′E) near Brisbane, Queensland, Australia. The animals were kept in individual plastic containers in the laboratory in Canberra for up to 6 weeks before experiments. During this period they were regularly provided with fresh seawater and fish food.

We took frontal macro-photographs of a total of 73 crabs from the two collection sites in several sessions in the field and the laboratory. The relationship of eye height, eye width, eye separation and eyestalk length to carapace width was analysed in a linear mixed model in R (R Development Core Team, Vienna, Austria) using experimental session as a random parameter and crab sex, carapace width and handedness (the side of the larger claw in males) as variables. Variables were only included in the model if they were significant ($P<0.05$) when added to the model last.

All optical measurements were performed on live and intact animals. To restrain the crabs, their legs and claws were tied together with tape. The males were forced to autotomise their larger claw by pinching the merus with forceps. An aluminium bar was then glued to the carapace and one eye stalk fixed to the bar with Blu-Tack and tape in an approximately natural position. During the experiment the eye was kept moist while taking care that no drops formed on the eye that would distort the microscope image. Using the attached aluminium bar, the crab was fixed with its eye upright in the rotation centre of a goniometer microscope (Fig. 1) (Dahmen, 1991). This allowed us to rotate the microscope along a horizontal and a vertical axis around the eye and thereby adjust its optical axis to different angles of azimuth and elevation. The microscope was fitted with a 1.3 megapixel USB camera to monitor focus, position the microscope and rapidly acquire images.

Optical measurements

We examined almost the whole equatorial and dorsal field of view in one large adult female (19 mm carapace width). Through the microscope, the principal pseudopupil (Franceschini, 1975; Stavenga, 1979) can be observed as a dark spot that follows the observer around the eye (Fig. 2, inset). It highlights the facets looking into the aperture of the microscope. By observing the position of the pseudopupil from many different angles around the eye, the optical axes of all ommatidia can thus be inferred (Franceschini, 1975). Our basic experimental approach was similar to that of several previous studies (Dahmen, 1991; Petrowitz et al., 2000). Starting at the medial rim of the eye, we took consecutive measurements, first every 5 deg. of azimuth along the eye equator (0 deg. elevation), and then along 13 vertical strips every 30 deg. of azimuth. Each strip included measurements at a maximum of 18 elevations in 5 deg. steps between –10 deg. and 70 deg. At each elevation we took three measurements with a horizontal offset of –5 deg., 0 deg. and 5 deg.
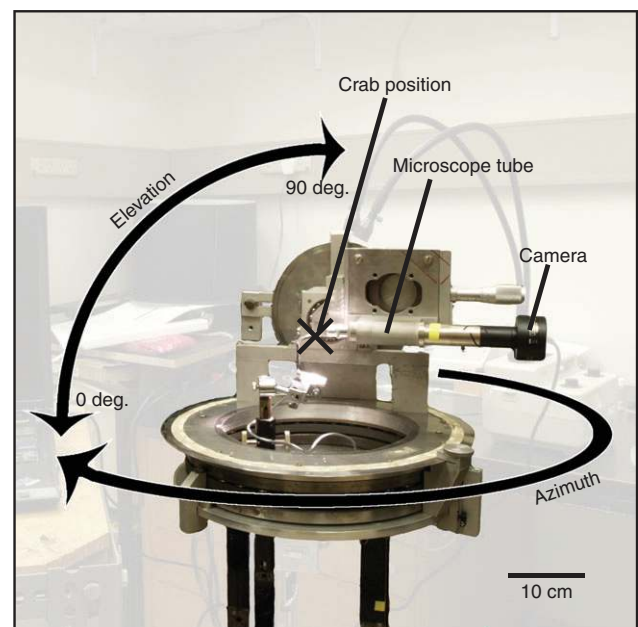

Fig. 1. Goniometer microscope (Dahmen, 1991), allowing for a microscope with attached digital camera to be rotated to defined angles of azimuth and elevation. The live but restrained crab was fixed in the rotation centre with its eye in a natural upright position. The frontal viewing direction was defined as 0 deg. azimuth, with angles increasing along the lateral visual field towards the rear. The visual horizon was defined as 0 deg. elevation with negative values in the ventral and positive values in the dorsal visual field.

azimuth, resulting in three adjacent vertical transects 5 deg. apart. Each one of the resulting 780 measurements consisted of two photographs: one at the level where the principal pseudopupil could be observed clearest, and one at the focus level of the facets. The large depth of field of our microscope allowed us to identify, count, measure and connect all facets between strips and thus directly account for a total of 6925 individual ommatidia. This produced a continuous map of ommatidia filling almost the entire dorsal and part of the ventral visual field.

The dorsal extent of the visual field was determined in the goniometer micrographs and then confirmed and extended to the full extent of the visual field in a different female crab. At the border of the visual field the pseudopupil suddenly broadens and merges into the rim of the ommatidial array, making it hard to reliably determine pseudopupil positions and reconstruct optical axes. To exclude these facets, we defined the border of the field of view as the last point at which we could identify a clear pseudopupil leading to a likely underestimation of the full field of view by about 10 deg. Selected parts of the visual field were measured in five additional animals (three males and two females with carapace widths between 14 mm and 22 mm). In three of these animals we took measurements along the eye equator and two vertical strips, one frontal (0 deg. azimuth), one lateral (90 deg. azimuth). In the other two we measured only the lateral strip. In all these additional crabs we reduced our minimum vertical step size to 1.25 deg. for increased measurement accuracy in the equatorial acute zone.

Measurements

In every photograph, the centres of all visible facets and of the pseudopupil were marked using custom-made software in MATLAB 7.4 (The MathWorks, Natick, MA, USA). We used natural irregularities in the eye to identify individual facets that were visible in adjacent images. With at least three such common facets for each pair of neighbouring images we could individually label all 6925 observed facets, relate them to their neighbours and combine them with the measured pseudopupil positions into a single map. Photographs were calibrated using images of a microscope calibration slide.

In most cases, the positions of the pseudopupil centres developed smoothly on this map, but some deviations were clearly visible. Especially near the eye equator, where the pseudopupil is large and tear shaped, its centre was often difficult to determine accurately. Similarly, in some parts of the dorsal eye the dark pigmentation made it hard to clearly identify facets and pseudopupils. We therefore adjusted the positions of our measured pseudopupil centres by smoothing their positional function using a two-dimensional thin-plate spline (Wahba, 1990). Great care was taken not to introduce artefacts during this procedure and all splined positions were projected back onto original images for visual confirmation.

Viewing directions could then be assigned to a total of 5132 ommatidia that lay within the grid of measured pseudopupils. The viewing direction of a facet at a pseudopupil centre is equal to the pseudopupil's 'viewing direction', i.e. the optical axis of the microscope when the pseudopupil was observed. For facets that lay between measured pseudopupils, we linearly interpolated between adjacent viewing directions.

Once an animal is fixed in the goniometer, the optics of the eye start degrading within hours, even when the eye and animal are constantly kept moist. A quick procedure is therefore essential, making it difficult to perfectly align the eye centrally and upright at the beginning of the experiment. In our final map, the acute zone of highest vertical resolution was sinusoidally modulated in a way

that could be fully explained by a 6 deg. tilt of the eye in the goniometer. Previous studies (Land and Layne, 1995a; Zeil and Al-Mutairi, 1996) have shown that under natural conditions crabs align this acute zone with the visual horizon. We therefore rotated our map accordingly to adjust for this tilt.

Analysis

We determined the partial interommatidial angle $\Delta\varphi$ (following Stavenga, 1979) in the vertical direction by calculating the distance between horizontal ommatidial rows, and in the horizontal direction as half the distance between ommatidia along these rows (Fig. 4E). Vertical and horizontal sampling resolution in cycles per degree (cycles deg.$^{-1}$) follow as $\nu_s = 1/(2\Delta\varphi)$.

The area of every facet was measured as the area of its Voronoi cell (the cell containing all points that are closer to this than to any other facet). We determined the facet diameter (D, in μm) from facet area (A, in μm^2) as the diameter of a round facet of equal area [$D = 2\sqrt{(A/\pi)}$; Fig. 5B]. In some parts of the eye facets were asymmetric, but the diameter along their largest dimension was never more than 10% larger than D. In a lens of diameter D, a point source of monochromatic light (wavelength λ) is blurred onto an area known as the Airy disc or Fraunhofer diffraction pattern with a full width at half maximum (FWHM) of $\Delta\rho_l = 1.02\lambda/D$. This half-width represents the part of an ommatidium's acceptance angle that is due purely to diffraction in the lens.

Due to waveguide effects, the full acceptance angles $\Delta\rho$ of ommatidia are not easily determined theoretically (Stavenga, 2003a; Stavenga, 2003b; Stavenga, 2004). However, the acceptance angle can be approximated by the half width $\Delta\rho_l$ of the Airy disc in three circumstances: when the eye is strongly light adapted, when the rhabdom is very thin and propagates mostly the fundamental waveguide mode, and/or when the focal lengths of the lenses are large compared with their diameters (Stavenga, 2003a; Stavenga, 2003b; Stavenga, 2004). In the case of *U. vomeris*, all these conditions are likely to be satisfied since these crabs are active in bright daylight only, they have rhabdoms that are extremely thin and their focal length is about 5–6 times larger than the lens diameter (Alkaladi, 2008). In this study, we have therefore used Airy disc half-widths to estimate acceptance angles.

Extrapolation to a full eye model

Apparatus and time constraints did not allow us to measure the full ventral visual field in our main animal. We therefore included the ventral part of the frontal and lateral strips that we had measured in a size-matched female. To achieve a full description of the *U. vomeris* sampling grid, we splined and extrapolated the functions describing the vertical distance between rows and the horizontal distance between facets. Parameters of the splines were carefully adjusted to smoothly continue observed resolution curves and, where known, approximate the total number of rows we had observed in the main female. Ommatidia were then consecutively added according to the smoothed functions until the visual field was filled to the rim. These extrapolations thus created a full model of the eye based on measurements from two females.

RESULTS
Eye morphology

The compound eyes of *U. vomeris* (Fig. 2, inset) are vertically elongated ellipsoids situated on long eyestalks at the front of the carapace. The ommatidial array wraps around the eyestalk, leaving only a narrow cuticular ridge free from ommatidia at the median surface of the eyestalk. In adult animals, the eyes are up to 2.3 mm

Table 1. Anatomical eye measurements increase linearly with body size

	β_1	β_2	β_3	Range (mm)	Res. d.f.
Eye length	0.844***	0.055***	0.063***	1.35–2.25	145
Eye width	0.632***	0.030***	0.068***	0.86–1.4	145
Stalk length	−0.378***	0.343***	0.270***	3.0–8.64	134
Eye separation	2.395***	0.166***	0 (P=0.16)	3.85–8.0	50

Frontal macro-photographs were taken of 74 crabs between 10 and 25 mm carapace width (cw) and anatomical parameters of both eyes were measured where possible. A linear mixed model was applied with crab and set-up as random effects. All parameters except eye separation are significantly larger in males. Regression lines are given by $\beta_1+\beta_2\times$cw$+\beta_3\times$sex, where sex is 0 for females and 1 for males. ***P<0.001.

high and 1.4 mm wide, and are held up to 8.6 mm above the carapace (Table 1). In a flat, natural environment, the eyestalks are held almost perfectly vertical, placing the centres of the eyes between 4 mm and 8 mm apart. All anatomical dimensions, including eye size, scale linearly with body size (Table 1, Fig. 2). Eyes and eyestalks are slightly, but significantly, larger in males; they are approximately equivalent to those of a 1–2 mm larger female.

Visual field

The field of view of each eye covers practically the entire visual space except for the ventral-most part, where the crab would see itself (Fig. 3). The ventral border of the sampling array thus essentially follows the outline of the animal's own body, limiting the field of view to −70 deg. of elevation in the frontal eye, −45 deg. in the lateral, −35 deg. in the posterior and less than −20 deg. in the medial part of the eye. Along the visual horizon (between −20 deg. and 40 deg. of elevation), the sampling array covers the full 360 deg. panorama. In fact, the two ends of the facet-bearing surface that meet at the medial cuticular ridge view the same region of visual space, creating a monocular overlap of at least 30 deg. Dorsally, the mapped visual field extends to about 70 deg. of elevation in the frontal and lateral eye, decreasing to 50 deg. at the back and even further towards the medial cuticular ridge. Contrary to what our maps (Figs 3–5) suggest, the dorsal visual field is most likely fully covered. However, we estimate the receptive fields of the border ommatidia to be more than 10 deg. in diameter. This makes their visual axes hard to determine and they are therefore not included in the maps.

Variation of sampling resolution

Despite this immense field of view, each eye only contains about 8000 ommatidia, each of which functions as a single 'pixel'. The severity of this restriction becomes apparent when one considers that even a simple, 1 megapixel digital camera has 125 times as many pixels, while sampling an approximately 15 times smaller visual field. This tension between coverage and resolution has led to the evolution of several distinct regional specialisations in this facet array. Most facets look into an extremely narrow band of visual space around the horizon (Zeil et al., 1986; Land and Layne, 1995a; Zeil and Al-Mutairi, 1996). In fact, one-third of all ommatidia are devoted to the central ±6.5 deg. of elevation. This is largely achieved through vertical elongation of the eye (Fig. 2 inset), leading to smaller vertical interommatidial angles and thus increased vertical sampling resolution (Fig. 4A,B). Outside of this horizontal acute zone, resolution declines steeply to a minimum of about 0.3 cycles deg.$^{-1}$ ventrally and 0.2 cycles deg.$^{-1}$ dorsally, i.e. just one facet every 2.5 deg. As we will see, the receptive fields of individual receptors in the ventral and dorsal visual field are much smaller than these interommatidial angles, resulting in severe undersampling.

Within the horizontal acute zone, there are two distinct areas of high resolving power: one views the frontal visual field (0 deg.) with a maximum resolution of 1.54 cycles deg.$^{-1}$, the second is situated laterally (60–90 deg.) with a maximum of 1.48 cycles deg.$^{-1}$. Away from these acute zones, resolution decreases along the horizon to a minimum of about 0.2 cycles deg.$^{-1}$ at the posterior–medial edge of
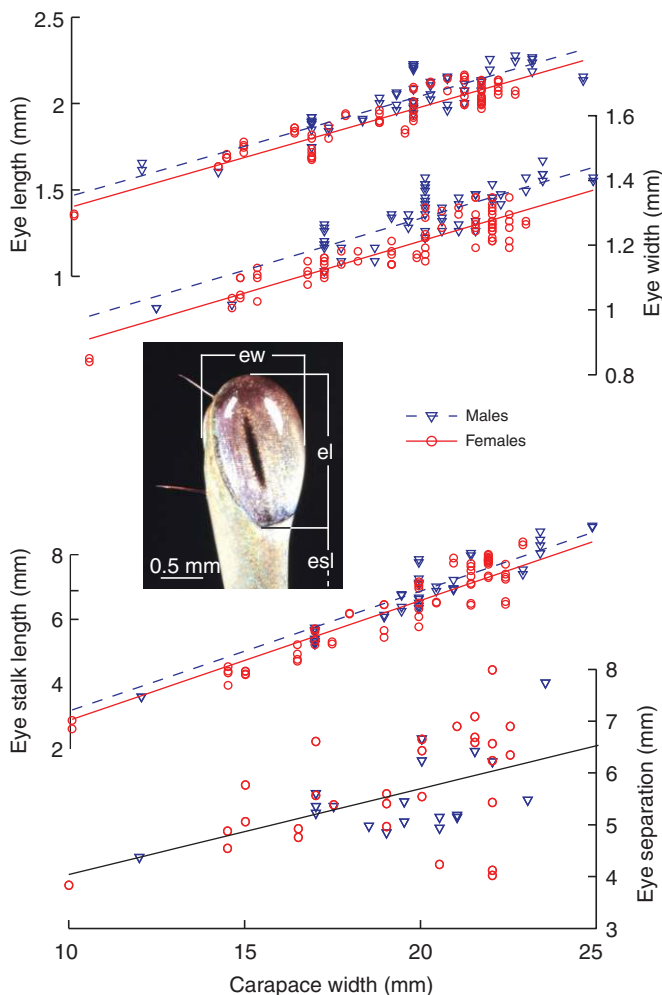

Fig. 2. Eye size as a function of body size and sex. Vertical eye length (el), horizontal eye width (ew), eye stalk length (esl, between the carapace and the lower end of the facet-bearing surface) and eye separation between centres, as measured in frontal macro-photographs, are plotted against carapace width for male (triangles) and female (circles) *Uca vomeris*. Regression lines are shown dashed for males and solid for females. All parameters depend significantly on carapace width and all measurements except eye separation are significantly larger in males (see Table 1).
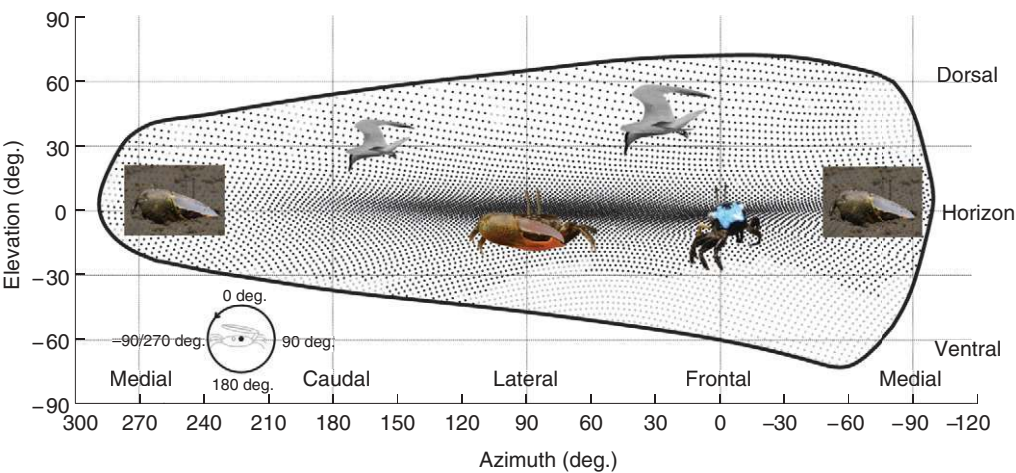
Fig. 3. Equirectangular map of the reconstructed optical axes of a *U. vomeris* female. Black dots represent observed facets, grey dots extrapolated facets. The rim of the visual field (thick black line) is defined at the last position where a clear pseudopupil can be observed, the total visual field is likely to be up to 10 deg. larger in all directions, but with a much lower density of optical axes. Inset images indicate relevant behavioural contexts in specialised areas: individual recognition frontally (female carapace pattern), burrow defence laterally (male with large claw), eye stalk alignment medially (crab on slope), predator avoidance dorsally (terns). See Discussion for details.

the sampling array (270 deg.). To test for the consistency of the difference between frontal and lateral peak resolution, we measured the number of facet rows inside the acute streak in all six examined animals. In the central ±20 deg. of elevation, frontal row counts (range 55–57) were always higher than lateral row counts (range 47–55; Table 2; Welch two-sample *t*-test, *t*=–5.32, d.f.=6.79, *P*<0.005). These numbers varied little even between animals of very different body size (see also Land and Layne, 1995a). Our final eye reconstruction (Fig. 3), in comparison, has 54 rows frontally and 52 laterally, values that are very close to the observed range. In a careful analysis of the combined data set from all six animals we determined the average frontal and lateral peak resolution to be 1.54 cycles deg.$^{-1}$ and 1.36 cycles deg.$^{-1}$, respectively (see Appendix).

Horizontal sampling resolution (Fig. 4C,D) is generally lower and more uniformly distributed than vertical resolution, with a shallow, broad peak of 0.45 cycles deg.$^{-1}$ at the lateral visual horizon (90 deg.). Resolution declines to 0.4 cycles deg.$^{-1}$ in the frontal eye (0 deg.), 0.35 cycles deg.$^{-1}$ in the rear (180 deg.) and to a minimum of around 0.25–0.3 cycles deg.$^{-1}$ in the far dorsal, ventral and medial parts of the eye (–90 deg./270 deg.).

Optical *vs* sampling resolution

In addition to the number of receptors per visual angle (sampling resolution), the resolving power of an eye is limited by the receptive fields of photoreceptors (angular sensitivity functions). The larger the receptive fields (usually described by their half width Δρ, the acceptance angle), the more blurred the image becomes. Contrast is thus reduced at higher spatial frequencies, up to the point at which no contrast remains at a spatial cut-off frequency $v_{co}=1/\Delta\rho$ [Sparrow limit (see Snyder, 1979; Warrant and McIntyre, 1993)]. Because of waveguide effects, Δρ values are not easily determined theoretically (Stavenga, 2003a; Stavenga, 2003b; Stavenga, 2004). However, in animals with long focal lengths, narrow rhabdoms and eyes that

generally work under bright light conditions – such as fiddler crabs – they can be approximated by the half-widths of Airy discs. These diffraction patterns describe the image of point-like light sources that reaches the photoreceptors (see Materials and methods) (Warrant and McIntyre, 1993). The size of these blur circles depends only on the diameter of the facet lenses and the wavelength of sampled light.

In *U. vomeris*, facets are largest at the eye equator, coinciding with the acute zone of highest vertical sampling resolution, but with a much broader distribution (Fig. 5A). In contrast to sampling resolution, facet diameters and therefore optical resolution are higher in the lateral than in the frontal visual field. The mean (±s.d.) facet diameter was 32.4±0.33 μm in the lateral visual field (*N*=80 in a 5 deg. radius around 90 deg. azimuth/0 deg. elevation) and 30.9±0.21 μm in the frontal visual field (*N*=54 in a 5 deg. radius around 0 deg. azimuth/–5 deg. elevation) (Welch two-sample *t*-test, *t*=–31.33, d.f.=131.56, *P*<0.001). The smallest facets we measured are in the far dorsal parts of the eye and are about 15 μm in diameter.

Note that the largest facets, and therefore the peak of optical resolution, in the frontal visual field are not at the visual horizon, but about 5 deg. ventrally (Fig. 5A). The area of highest contrast sensitivity thus points into a direction that would normally view the body of another crab about 10 cm away. This agrees well with evidence on the functional significance of this zone in social interactions (see Discussion).

According to information theory, the acceptance angles in an ideal imaging system should just cover visual space with minimal overlap (see Land, 1981; Warrant and McIntyre, 1993). If they are larger than this, information will be lost and the effective resolution will be limited by diffraction rather than by the sampling array. Conversely, if acceptance angles are smaller, visual space will be undersampled, i.e. there will be gaps in the field of view. In *U. vomeris*, Airy discs are clearly much smaller than interommatidial

Table 2. Horizontal ommatidial row counts compared between experimental animals and final model of the eye

		Total rows	Range	±20 deg. rows	Range	*N*
Measured	Frontal	89.7	86–93	56	55–57	3
	Lateral	73.6	65–79	49.3	47–55	6
Model	Frontal	79	–	54	–	–
	Lateral	69	–	52	–	–

Rows were counted as total number of horizontal rows along two vertical transects (lateral and frontal eye surface) and as number of rows between the pseudopupils at +20 deg. and –20 deg. of elevation. See Materials and methods.
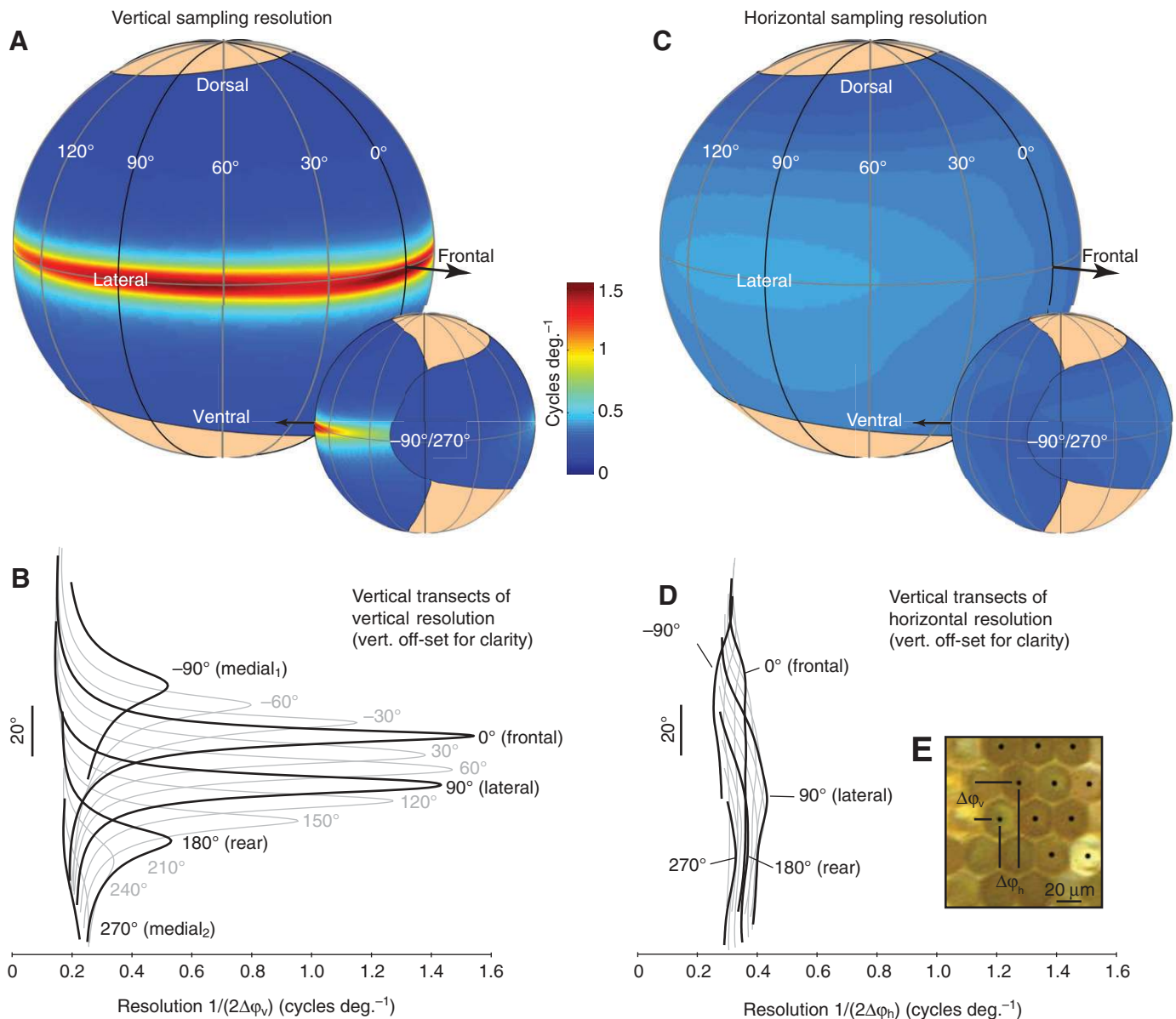
Fig. 4. Variation of sampling resolution across the eye. Vertical (A,B) and horizontal (C,D) sampling resolution (in cycles deg.$^{-1}$) on spherical maps from a fronto-lateral (A,C) and medial (insets) point of view and as vertical transects (B,D, vertically off-set for clarity). Transects, as well as meridians on the spherical maps, are shown every 30 deg. (grey lines) and emphasised every 90 deg. (black lines). Resolution was determined from partial interommatidial angles (E) measured as the angular distance between rows ($\Delta\varphi_v$: vertical resolution) and half the horizontal angular distance between facets in these rows ($\Delta\varphi_h$: horizontal resolution). Note the two distinct peaks (frontal and lateral) in the horizontal visual streak of vertical resolution. Horizontal resolution is up to four times lower at the horizon, but about 50% larger than vertical resolution in the dorsal and ventral visual field. Note that the medial visual field is sampled by both the fronto-medial (−90 deg.) and the posterior–medial (270 deg.) part of the facet-bearing surface.

angles in most of the visual field, suggesting drastic undersampling (Fig. 5C,D) (Dahmen, 1991; Zeil and Al-Mutairi, 1996). There are some regions of space that are effectively not sampled at all. Only at the horizon is visual space fully covered with little overlap of acceptance angles (Fig. 5E, shown for 400 nm light). However, acceptance angles increase linearly with the wavelength of transmitted light. A direct comparison between sampling and optical resolution for different wavelengths (Fig. 6) suggests that – in our relatively large study female – the frontal peak of sampling resolution can only be fully utilized for ultraviolet light. For longer wavelengths, resolution will be limited by diffraction. This effect will be reduced in larger animals and exaggerated in smaller animals.

DISCUSSION

We used a pseudopupil method to create a full map of sampling and optical resolution in the compound eyes of the fiddler crab *U. vomeris*. Our results show *U. vomeris* to be an extreme example of a flat-world crab, featuring long, very narrowly separated eyestalks and the most highly developed and narrowest visual streak described so far (Zeil et al., 1986; Land and Layne, 1995a; Zeil and Al-Mutairi, 1996).

The visual information zones

Because of the physiological costs of developing and maintaining a large eye (Niven and Laughlin, 2008), eye space is a valuable
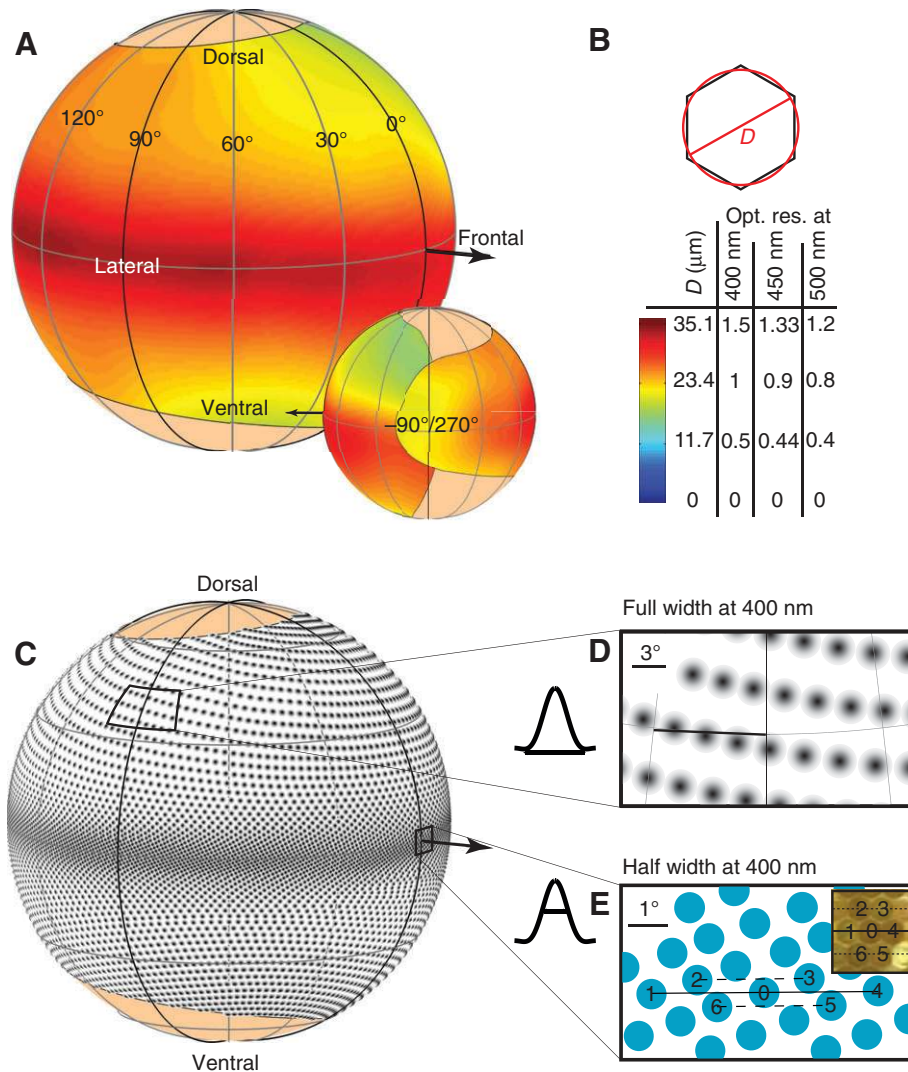
Fig. 5. Variation of optical resolution across the eye. (A) Spherical maps of facet diameter in a female *U. vomeris* (carapace width 19 mm) seen from fronto-lateral and medial (inset) points of view. Facet diameter was determined from the measured facet area as the diameter of a round facet of equal area (B). Optical resolution is directly proportional to the ratio of the wavelength of light to the facet diameter, and is listed for three example wavelengths beside the colour bar coding facet diameter. (C) Spherical map of receptive fields seen from the fronto-lateral point of view calculated for 400 nm light. (D) Magnification of a part of the dorsal visual field showing full Airy discs, representing receptive fields of ommatidia. There is considerable undersampling of the visual field. (E) Magnification of the fronto-equatorial visual field showing acceptance angles (half-width of receptive fields). The seven numbered ommatidia show how the row structure on the eye translates into visual space. For a perfect match of vertical sampling and optical resolution, next-but-neighbour facets (e.g. nos 2 and 6) should show no vertical overlap. The fact that they do overlap demonstrates that even for 400 nm light, vertical resolution in the frontal acute zone is diffraction limited in an animal of this size (see also Fig. 6A).

physiological resource. In this context, the regional specialisations of the sampling array we describe here can be interpreted as a heavily constrained optimisation of the use of eye space. For an eye to collect information efficiently, it should (i) direct more eye space towards more important regions of the visual field and (ii) within these zones trade off different uses of the available eye space (e.g. facet number *vs* facet size) depending on the nature of the information that is relevant in that region of the visual field. In this context, we will discuss five specialised regions of the *U. vomeris* compound eye (Fig. 3).

Ventral zone

In the ventral visual field, vertical sampling resolution decreases steeply away from the horizon to a minimum of about 0.3 cycles deg.$^{-1}$. This gradient seems to follow an inverse sine function, resulting in size constancy (Zeil et al., 1986; Schwind, 1989; Dahmen, 1991). In a flat environment, a distant object on the ground is seen at the horizon. As it comes closer, the lower edge of its retinal image moves downwards away from the visual horizon. At the same time it subtends an increasingly large visual angle, but is sampled at lower resolution. If vertical interommatidial angles $\Delta\varphi_v$ vary with the sine of elevation θ as $\Delta\varphi_v = \tan^{-1}(s/h) \times \sin(\theta)$, this will result in **size constancy**: an

object at a fixed height above ground will be sampled by the same number of ommatidia irrespective of its distance (Zeil et al., 1986; Schwind, 1989; Dahmen, 1991). The only parameter adjusted in this fit is the linear scaling constant $\tan^{-1}(s/h)$, the arctangent of the size s (in cm) of an object at height h (relative to eye height, in cm) that is projected onto one interommatidial angle. Our results confirm this hypothesis (Fig. 7). The inverse sine functions fit astonishingly well using the same value for s/h (0.11) in the latero-ventral, latero-dorsal and fronto-dorsal eye, but require a smaller value for s/h (0.09), corresponding to generally higher resolution, in the fronto-ventral visual field (Zeil and Al-Mutairi, 1996). For perfect size constancy, resolution would have to be infinitely large at the horizon. Size constancy therefore breaks down at about ±5 deg. Objects closer to the horizon (i.e. further away from the observer) appear smaller on the retina. In addition to simplifying the estimation of a conspecific's body size, size constancy has important consequences for the **detection of social signals**. It means that the vertical part of a conspecific's back pattern will look exactly the same no matter how far away that crab is, as long as it is closer than about 9–18 cm (see 'Frontal zone' below). A similar size constancy will of course be achieved in the dorsal visual field for horizontally flying birds when they are seen at equivalent elevations.
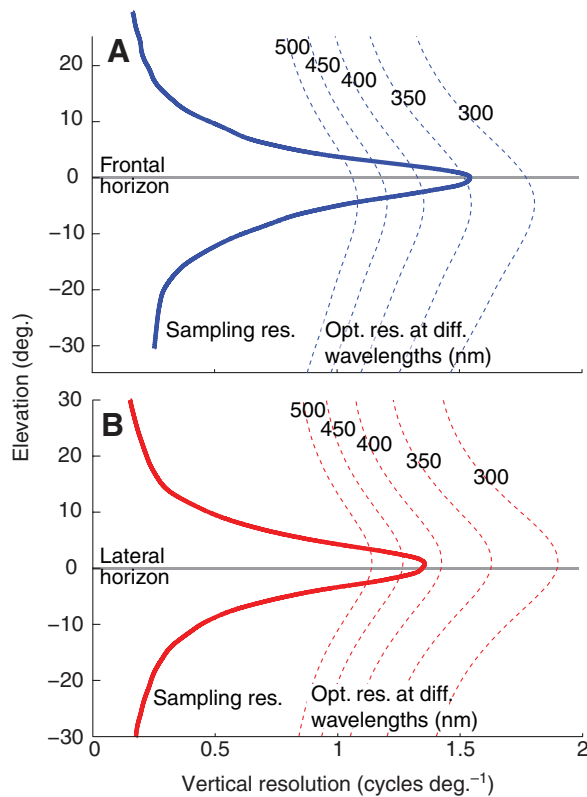
Fig. 6. Comparison of vertical sampling resolution (solid lines) and optical resolution (dashed lines) of *U. vomeris*. Sampling resolution was determined from averaged pseudopupil measurements in six animals along a lateral (A) and a frontal (B) transect (see Appendix). Optical resolution is expressed as cut-off frequency and was determined from lens diameters (Fig. 4) measured in a female crab (carapace width 19 mm). Optical resolution depends on the wavelength of sampled light and is shown for five different wavelengths. Note that the peak of optical but not sampling resolution is shifted by about 5 deg. below the horizon in the frontal visual field (since facet diameters are maximal at this location).
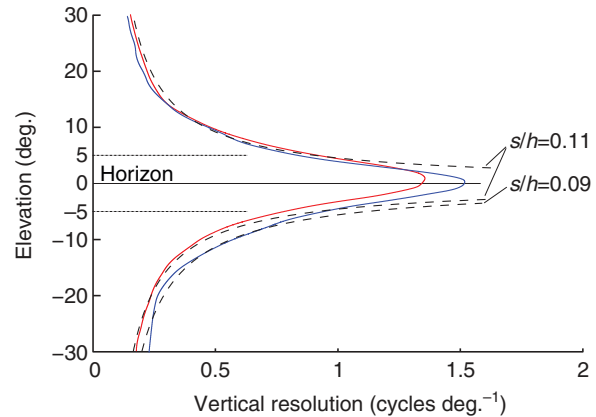

Fig. 7. Vertical sampling resolution profile results in size constancy. The decline of vertical sampling resolution (frontal blue, lateral red) can be predicted by an inverse sine function assuming that objects at constant height above ground are sampled by the same number of ommatidia irrespective of their distance (dashed lines). Functions can be scaled by a single parameter s/h (indicated beside the fits). See text for details.

Dorsal zone

The dorsal visual field is characterised by particularly low sampling resolution, yet comparatively high optical resolution, resulting in **severe undersampling**. As in the ventral visual field, vertical sampling resolution declines steeply with increasing elevation, following the same inverse sine function as in the ventral visual field. In the far dorsal visual field, a minimum of 0.2 cycles deg.$^{-1}$ is reached, resulting in a lower vertical than horizontal resolution. Facet diameters do not decrease at the same rate and the minimum facet diameter of about 15 μm results in an optical resolution several times larger than the vertical sampling resolution. Visual space is thus sampled by small receptive fields with large gaps between neighbouring viewing directions (Fig. 5D). This effect is not restricted to the highest elevations. At 10 deg. elevation, optical resolution is already more than twice as good as vertical sampling resolution (Fig. 6).

The simplest explanation for this undersampling is that 15 μm represents a minimum functional lens size and that therefore only a widely spaced facet array can cover the entire visual space. This structural explanation, however, is doubtful as some small insects have facets as small as 8 μm (Barlow, 1952). An alternative, functional hypothesis is suggested by the visual ecology of the crabs

(Zeil and Hemmi, 2006). The most important task in the dorsal visual field is the early detection of predators. Fiddler crabs will start dashing home towards the safety of their burrow when birds subtend a visual angle of only 1–2 deg. (Land and Layne, 1995a; Hemmi, 2005a). The task of the visual system is therefore not to extract detailed image information but to detect birds as early as possible against a very bright, uniform background. Neither high sampling resolution nor seamless coverage of the visual field is necessary for this task. However, small acceptance angles and high contrast sensitivity, as provided by comparatively large facets, are essential for **early predator detection**. In other words, the crabs sacrifice a continuous sampling of the dorsal visual field for a higher contrast and signal-to-noise ratio (e.g. Zeil, 1983) and therefore a larger, safer detection distance (Land, 1981; Zeil, 1983).

Frontal zone

In contrast to the ventral and dorsal areas discussed so far, the frontal and lateral horizontal parts of the visual field comprise the majority of eye space. These two high-resolution areas utilise this space with a different trade-off between facet number and size. In the frontal visual field the balance is biased towards more rather than larger facets, resulting in the overall **highest sampling resolution**, but comparatively lower optical resolution. Because of this trade-off, resolution is diffraction limited for long wavelength signals (Fig. 6A). The actual cut-off wavelength (350 nm for our 19 mm female) depends linearly on the size of the eye and thus on the size of the crab. Even in very large animals, though, the full sampling resolution can only be utilised for blue/UV signals or by short wavelength-sensitive photoreceptors. Indeed, we recently discovered a UV-sensitive photoreceptor class in *U. vomeris* using intracellular electrophysiology (Smolka, 2009), and behavioural evidence suggests that this frontal zone is involved in the analysis of short wavelength patterns. In *U. capricornis*, males recognise individual females by their carapace patterns (Detto et al., 2006) and in *U. vomeris* these patterns contain strong blue and UV components (Hemmi et al., 2006). When confronted with an approaching female, both *U. perplexa* (How et al., 2007) and *U. pugilator* (Land and Layne, 1995b) re-orient to face the female frontally. Approaching males, in contrast, are always kept laterally,

predominantly on the side of the major claw. Interestingly, this sex discrimination occurs at a distance of about 10–15 cm (Land and Layne, 1995b).

Our results complement these observations in several ways. Firstly, sampling resolution is highest in the frontal visual field for any given elevation below the horizon (i.e. for any given distance of an approaching crab). This is because the gradient of decay of vertical sampling resolution is shallowest in the frontal eye. Secondly, the frontal peak of optical resolution is at about –5 deg. below the visual horizon. On flat ground this corresponds to looking at the top of another crab's carapace at a distance of about 9 cm or at the bottom edge of the carapace of a crab at about twice that distance; –5 deg. of elevation is also where size constancy begins (see above). Together, these factors are likely to significantly reduce the neural complexity of the underlying pattern-matching task. The frontal eye region is thus the zone best equipped for **recognising individual conspecifics**. It is therefore plausible that the re-orientation behaviour of courting males not only directs the waving signal towards the target female but also centres her on his frontal acute zone.

Lateral zone
In contrast to the frontal visual field, the lateral zone has larger rather than more facets, leading to the **highest contrast sensitivity** and optical resolution. Horizontal resolution is also highest in this part of the visual field. During normal foraging excursions, fiddler crabs always align their longitudinal body axis with the direction of their burrow (Land and Layne, 1995b; Zeil, 1998; Zeil and Layne, 2002; How et al., 2007). When another crab approaches, the resident rushes back to defend its burrow from the intruder (Crane, 1975; Zeil and Layne, 2002; Hemmi and Zeil, 2003a; Hemmi and Zeil, 2003b). Interestingly, this decision is made when the intruding crab is a fixed distance away from the burrow (Hemmi and Zeil, 2003c). The crabs that are furthest away – often in excess of 50 cm at the time of response (Hemmi and Zeil, 2003b) – and thus hardest to detect, are consequently seen across the burrow in the lateral visual field. To reliably **detect intruding crabs** and accurately measure their position relative to the burrow, both high contrast sensitivity and high vertical resolution are essential. The different trade-off between facet size and interommatidial angles, when compared with the frontal zone, enhances the crabs' ability to detect small contrast changes. In addition, it means that in the lateral visual field the full resolution can be used at longer wavelengths of light without being limited by lens diffraction. A large crab can thus optimally sample practically the whole range of wavelengths to which *U. vomeris* photoreceptors are sensitive, up to about 550 nm (Fig. 6B) (Jordão et al., 2007; Smolka, 2009).

Medial zone
Despite the fact that the medial cuticular ridge forms an anatomical gap in the ommatidial array, the visual field at the horizon is fully covered. In fact, the visual fields of the two ends of the eye surface create a **monocular overlap** of at least 30 deg. (Zeil and Al-Mutairi, 1996). What is the function of this medial region, where horizontal and vertical resolution are very low and facets small, especially when compared with the lateral part of the opposite eye, which looks into the same region of visual space?

One function of this monocular overlap might be to ensure full panoramic vision even under monocular viewing conditions (Zeil and Al-Mutairi, 1996). Before leaving their burrow after escaping from a perceived threat, crabs frequently sit in the burrow entrance and cautiously raise one eye while the rest of the body remains hidden. It is essential for this '**periscope strategy**' that the monocular visual fields cover the full panorama. This does not, however, explain the large extent of the 30 deg. monocular overlap. The distance between pseudopupils that look into the same visual angle from the two sides of the ridge is about 0.5 mm. A simple calculation (Burkhardt et al., 1973) shows that the maximum distance for stereoptic depth perception with a horizontal interommatidial angle of 3–4 deg. is between 7 mm and 9.5 mm. Under normal circumstances, the only object within this distance is the other eye. In a natural environment, crabs keep the vertical axis of their eyes perpendicular to the visual horizon (Zeil and Al-Mutairi, 1996) using visual and statocyst reflexes (Nalbach et al., 1989), even when the body is tilted at a large angle [e.g. on a slanted surface or in the burrow entrance (Zeil et al., 1989; Zeil, 1990)]. We thus suggest that the medial monocular overlap monitors the position and distance of the opposite eye to help with **aligning the visual fields** of the two eyes.

CONCLUSIONS
This study provides evidence that behavioural strategies and the design of sensory systems co-evolved to facilitate the extraction of ecologically relevant sensory information. Our results demonstrate that it is essential to understand the flow and processing of natural information under behaviourally relevant conditions in order to interpret the evolution and ecology of animals, their nervous systems and their behaviour.

APPENDIX
Detailed analysis of frontal and lateral resolution profiles
The width and height of the resolution peak depend critically on the exact measurement of the movement of a large pseudopupil within a very small angular movement of the microscope. For instance, the pseudopupil of the eye pictured in Fig. 2 (inset) spans about 40 facet rows. An error in the estimation of its centre by just one facet could lead to an error in peak resolution of 0.1 cycles deg.$^{-1}$. To more accurately estimate peak height and width and the difference between the lateral and frontal visual field, we repeated the measurements, with increased accuracy, along frontal and lateral transects in an additional three and five animals, respectively. Although these animals were of different sizes (14–22 mm carapace width), corresponding resolution profiles were very similar across animals (Fig. A1A). We thus averaged pseudopupil positions over all five animals. Pseudopupil elevation increases with the facet row that coincides with the pseudopupil centre in an inverse sigmoidal relationship (Fig. A1A). We shifted the centre of this curve (which determines the peak of vertical resolution) to coincide in all animals and then fitted a spline through this curve (separately for frontal and lateral visual fields). The stiffness of this spline critically determines the height and shape of the resulting resolution curve (Fig. A1B, solid lines). At high stiffness the fit is practically linear through the data points resulting in a flat resolution profile and large spline residuals. With decreasing stiffness the spline follows the data more closely and the shape that the spline forces onto the resolution profile is reduced (Fig. A1B, dashed line). As a consequence, peak resolution increases until at very low stiffness the curve becomes less smooth and develops secondary peaks due to small variances in the data (Fig. A1B, dotted line). Importantly, irrespective of stiffness, the frontal peak resolution was always higher than the lateral resolution. Using an intermediate stiffness value (0.8, Fig. A1B) we finally obtained an average peak resolution of 1.54 cycles deg.$^{-1}$ frontally and 1.36 cycles deg.$^{-1}$ laterally (Fig. A1C).
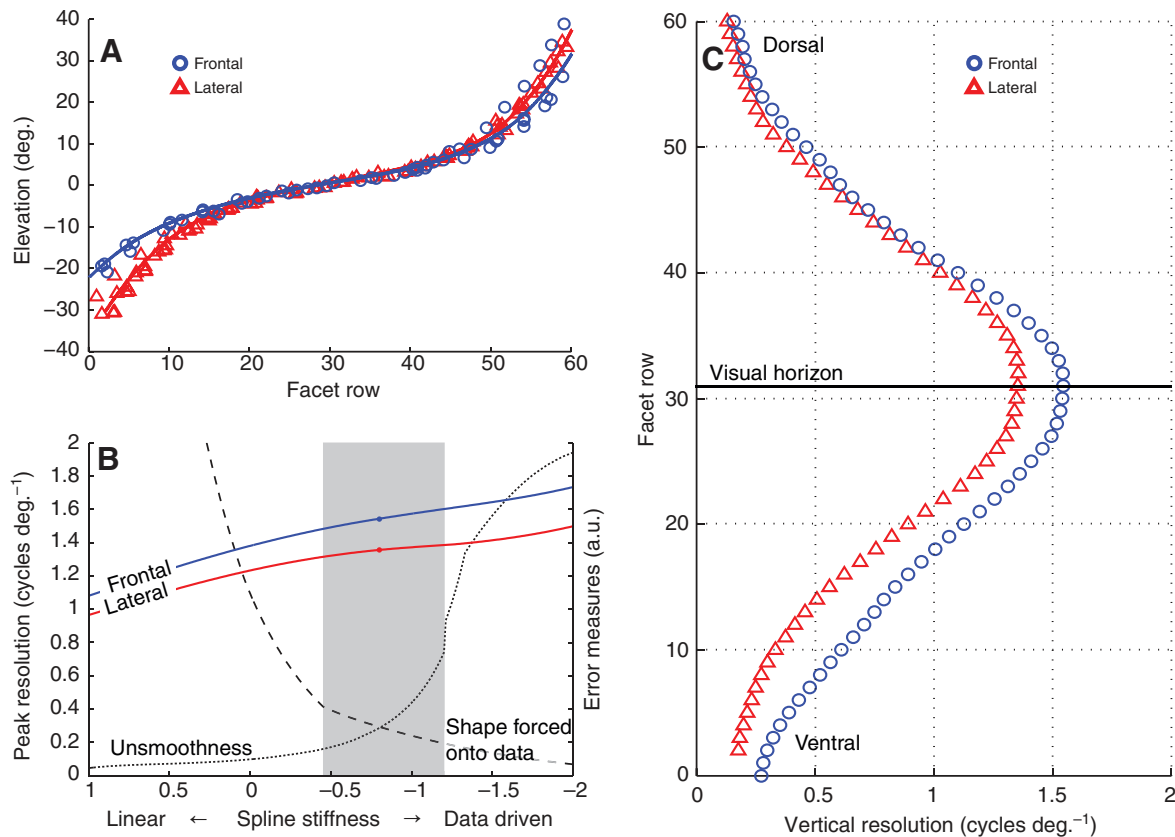
Fig. A1. Detailed analysis of frontal and lateral resolution profiles. (A) Centre positions of pseudopupils measured along a vertical transect in the frontal (circles) and lateral (triangles) visual field of six *U. vomeris* (three males, three females, carapace width 14–22 mm). Facet row numbers are arbitrary and were shifted to overlie smoothed 0 deg. pseudopupil positions. Positions were fitted with a thin-plate spline using a large range of stiffness constants (here shown for –0.8 in the units of B). To adjust for lower measurement accuracy, stiffness was linearly increased with distance from 0 deg. elevation. (B) Maximum resolution (solid lines) resulting from splines with different stiffness constants. Two error measurements (arbitrary units, a.u.) characterise the goodness of fit (dashed and dotted lines, see text for explanation). Note that in the range where both errors are acceptable (grey bar), peak resolution hardly changes, and that frontal resolution is always higher than lateral resolution. (C) Vertical sampling resolution resulting from a spline with stiffness constant –0.8 over facet row. Individual points represent individual facets along a vertical transect.

REFERENCES

Alkaladi, A. (2008). The functional anatomy of the fiddler crab compound eye. PhD Thesis. Canberra: The Australian National University.

Altevogt, R. and von Hagen, H. O. (1964). Über die Orientierung von *Uca tangeri* (Eydoux) im Freiland. *Z. Morph. Ökol. Tiere* **53**, 636-656.

Arikawa, K. (2003). Spectral organization of the eye of a butterfly, *Papilio. J. Comp. Physiol. A* **189**, 791-800.

Barlow, H. B. (1952). The size of ommatidia in apposition eyes. *J. Exp. Biol.* **29**, 667-674.

Burkhardt, D., Darnhofer-Demar, B. and Fischer, K. (1973). Zum binokularen Entfernungssehen der Insekten. *J. Comp. Physiol. A* **87**, 165-188.

Burton, B. G., Tatler, B. W. and Laughlin, S. B. (2001). Variations in photoreceptor response dynamics across the fly retina. *J. Neurophysiol.* **86**, 950-960.

Crane, J. (1975). *Fiddler Crabs Of The World (Ocypodidae: Genus Uca)*. Princeton, NJ: Princeton University Press.

Dacke, M., Nordstrom, P. and Scholtz, C. H. (2003). Twilight orientation to polarised light in the crepuscular dung beetle *Scarabaeus zambesianus. J. Exp. Biol.* **206**, 1535-1543.

Dahmen, H. J. (1991). Eye specialisation in waterstriders: an adaptation to life in a flat world. *J. Comp. Physiol. A* **169**, 623-632.

Detto, T., Backwell, P. R. Y., Hemmi, J. M. and Zeil, J. (2006). Visually mediated species and neighbour recognition in fiddler crabs (*Uca mjoebergi* and *Uca capricornis*). *Proc. R. Soc. Lond. B* **273**, 1661-1666.

Detto, T., Hemmi, J. M. and Backwell, P. R. Y. (2008). Colouration and colour changes of the fiddler crab, *Uca capricornis*: a descriptive study. *PLoS ONE* **3**, e1629.

Eckert, M. P. and Zeil, J. (2001). Towards an ecology of motion vision. In *Motion Vision: Computational, Neural, and Ecological Constraints* (ed. J. M. Zanker and J. Zeil), pp. 333-369. Berlin, Heidelberg, New York: Springer Verlag.

Franceschini, N. (1975). Sampling of the visual environment by the compound eye of the fly: fundamentals and applications. In *Photoreceptor Optics* (ed. A. W. Snyder and R. Menzel), pp. 98-125. Berlin, Heidelberg, New York: Springer.

Gibson, J. J. (1950). *The Perception Of The Visual World.* Cambridge: Riverside.

Hemmi, J. M. (2005a). Predator avoidance in fiddler crabs. 1. Escape decisions in relation to the risk of predation. *Anim. Behav.* **69**, 603-614.

Hemmi, J. M. (2005b). Predator avoidance in fiddler crabs. 2. The visual cues. *Anim. Behav.* **69**, 615-625.

Hemmi, J. M. and Zeil, J. (2003a). Burrow surveillance in fiddler crabs. I. Description of behaviour. *J. Exp. Biol.* **206**, 3935-3950.

Hemmi, J. M. and Zeil, J. (2003b). Burrow surveillance in fiddler crabs. II. The sensory cues. *J. Exp. Biol.* **206**, 3951-3961.

Hemmi, J. M. and Zeil, J. (2003c). Robust judgement of inter-object distance by an arthropod. *Nature* **421**, 160-163.

Hemmi, J. M. and Zeil, J. (2005). Animals as prey: perceptual limitations and behavioural options. *Mar. Ecol. Prog. Ser.* **287**, 274-278.

Hemmi, J. M., Marshall, J., Pix, W., Vorobyev, M. and Zeil, J. (2006). The variable colours of the fiddler crab *Uca vomeris* and their relation to background and predation. *J. Exp. Biol.* **209**, 4140-4153.

How, M. J. and Hemmi, J. M. (2008). Courtship herding in the fiddler crab *Uca elegans. J. Comp. Physiol. A* **194**, 1053-1061.

How, M. J., Zeil, J. and Hemmi, J. M. (2007). Differences in context and function of two distinct waving displays in the fiddler crab, *Uca perplexa* (Decapoda: Ocypodidae). *Behav. Ecol. Sociobiol.* **62**, 137-148.

Hughes, A. (1977). The topography of vision in mammals of contrasting life style: comparative optics and retinal organisation. In *Handbook Of Sensory Physiology*, vol. VII/5 (ed. H. Autrum), pp. 613-756. Berlin, Heidelberg, New York: Springer.

Jordão, J. M., Cronin, T. W. and Oliveira, R. F. (2007). Spectral sensitivity of four species of fiddler crabs (*Uca pugnax, Uca pugilator, Uca vomeris* and *Uca tangeri*) measured by *in situ* microspectrophotometry. *J. Exp. Biol.* **210**, 447-453.

Körding, K. P., Kayser, C., Einhauser, W. and Konig, P. (2004). How are complex cell properties adapted to the statistics of natural stimuli? *J. Neurophysiol.* **91**, 206-212.

Krapp, H. G. and Hengstenberg, R. (1996). Estimation of self-motion by optic flow processing in single visual interneurons. *Nature* **384**, 463-466.

Labhart, T. (1980). Specialized photoreceptors at the dorsal rim of the honeybee's compound eye: polarizational and angular sensitivity. *J. Comp. Physiol. A* **141**, 19-30.

Land, M. F. (1981). Optics and vision in invertebrates. In *Handbook Of Sensory Physiology*, vol. VII/6B (ed. H. Autrum), pp. 471-592. Berlin, Heidelberg, New York: Springer.

Land, M. F. (1989). Variations in the structure and design of compound eyes. In *Facets Of Vision* (ed. D. G. Stavenga and R. C. Hardie), pp. 90-111. Berlin, Heidelberg, New York: Springer.

Land, M. F. (1999). The roles of head movements in the search and capture strategy of a tern (Aves, Laridae). *J. Comp. Physiol. A* **184**, 265-272.

Land, M. F. and Layne, J. E. (1995a). The visual control of behavior in fiddler crabs. 1. Resolution, thresholds and the role of the horizon. *J. Comp. Physiol. A* **177**, 81-90.

Land, M. F. and Layne, J. E. (1995b). The visual control of behavior in fiddler crabs. 2. Tracking control systems in courtship and defense. *J. Comp. Physiol. A* **177**, 91-103.

Layne, J. E., Barnes, W. J. P. and Duncan, L. M. J. (2003a). Mechanisms of homing in the fiddler crab *Uca rapax*. 1. Spatial and temporal characteristics of a system of small-scale navigation. *J. Exp. Biol.* **206**, 4413-4423.

Layne, J. E., Barnes, W. J. P. and Duncan, L. M. J. (2003b). Mechanisms of homing in the fiddler crab *Uca rapax*. 2. Information sources and frame of reference for a path integration system. *J. Exp. Biol.* **206**, 4425-4442.

Loew, E. R. and Lythgoe, J. N. (1985). The ecology of colour vision. *Endeavour* **9**, 170-174.

Lythgoe, J. N. and Partridge, J. C. (1989). Visual pigments and the acquisition of visual information. *J. Exp. Biol.* **146**, 1-20.

Marshall, J., Cronin, T. W. and Kleinlogel, S. (2007). Stomatopod eye structure and function: a review. *Arthropod Struct. Dev.* **36**, 420-448.

Nalbach, H. O., Zeil, J. and Forzin, L. (1989). Multisensory control of eye-stalk orientation in space: crabs from different habitats rely on different senses. *J. Comp. Physiol. A* **165**, 643-649.

Niven, J. E. and Laughlin, S. B. (2008). Energy limitation as a selective pressure on the evolution of sensory systems. *J. Exp. Biol.* **211**, 1792-1804.

Petrowitz, R., Dahmen, H., Egelhaaf, M. and Krapp, H. G. (2000). Arrangement of optical axes and spatial resolution in the compound eye of the female blowfly *Calliphora. J. Comp. Physiol. A* **186**, 737-746.

Schwind, R. (1989). Size and distance perception in compound eyes. In *Facets Of Vision* (ed. D. G. Stavenga and R. C. Hardie), pp. 425-444. Berlin, Heidelberg, New York: Springer Verlag.

Simoncelli, E. P. and Olshausen, B. A. (2001). Natural image statistics and neural representation. *Annu. Rev. Neurosci.* **24**, 1193-1216.

Smolka, J. (2009). Sampling visual space: topography, colour vision and visually guided predator avoidance in fiddler crabs (*Uca vomeris*). PhD Thesis. Canberra: The Australian National University.

Snyder, A. W. (1979). Physics of vision in compound eyes. In *Handbook Of Sensory Physiology*, vol. VII/6A (ed. H. Autrum), pp. 225-313. Berlin, Heidelberg, New York: Springer.

Sparks, D. L. (2005). An argument for using ethologically "natural" behaviors as estimates of unobservable sensory processes. Focus on "Sound localization performance in the cat: the effect of restraining the head". *J. Neurophysiol.* **93**, 1136-1137.

Srinivasan, M. V. (1993). How insects infer range from visual motion. *Rev. Oculomot. Res.* **5**, 139-156.

Stavenga, D. G. (1979). Pseudopupils of compound eyes. In *Handbook Of Sensory Physiology*, vol. VII/6a (ed. H. Autrum), pp. 357-439. Berlin, Heidelberg, New York: Springer.

Stavenga, D. G. (2003a). Angular and spectral sensitivity of fly photoreceptors. I. Integrated facet lens and rhabdomere optics. *J. Comp. Physiol. A* **189**, 1-17.

Stavenga, D. G. (2003b). Angular and spectral sensitivity of fly photoreceptors. II. Dependence on facet lens F-number and rhabdomere type in *Drosophila. J. Comp. Physiol. A* **189**, 189-202.

Stavenga, D. G. (2004). Angular and spectral sensitivity of fly photoreceptors. III. Dependence on the pupil mechanism in the blowfly *Calliphora. J. Comp. Physiol. A* **190**, 115-129.

von Hagen, H. O. (1967). Nachweis einer kinästethischen Orientierung bei *Uca rapax. Z. Morph. Ökol. Tiere* **58**, 301-320.

Wahba, G. (1990). *Spline Models For Observational Data.* Philadelphia: Society for Industrial and Applied Mathematics.

Walls, G. L. (1942). *The Vertebrate Eye And Its Adaptive Radiation.* Bloomfield Hills, MI: Cranbook Press.

Warrant, E. J. and McIntyre, P. D. (1993). Arthropod eye design and the physical limits to spatial resolving power. *Prog. Neurobiol.* **40**, 413-461.

Zeil, J. (1983). Sexual dimorphism in the visual system of flies: The compound eye and neural superposition in *Bibionidae* (Diptera). *J. Comp. Physiol. A* **150**, 379-393.

Zeil, J. (1990). Substratum slope and the alignment of acute zones in semiterrestrial crabs (*Ocypode ceratophthalmus*). *J. Exp. Biol.* **152**, 573-576.

Zeil, J. (1998). Homing in fiddler crabs (*Uca lactea annulipes* and *Uca vomeris*: Ocypodidae). *J. Comp. Physiol. A* **183**, 367-377.

Zeil, J. and Al-Mutairi, M. M. (1996). The variation of resolution and of ommatidial dimensions in the compound eyes of the fiddler crab *Uca lactea annulipes* (Ocypodidae, Brachyura, Decapoda). *J. Exp. Biol.* **199**, 1569-1577.

Zeil, J. and Hemmi, J. M. (2006). The visual ecology of fiddler crabs. *J. Comp. Physiol. A* **192**, 1-25.

Zeil, J. and Layne, J. E. (2002). Path integration in fiddler crabs and its relation to habitat and social life. In *Crustacean Experimental Systems in Neurobiology* (ed. K. Wiese), pp. 227-246. Berlin, Heidelberg, New York: Springer.

Zeil, J., Nalbach, G. and Nalbach, H. O. (1986). Eyes, eye stalks and the visual world of semi-terrestrial crabs. *J. Comp. Physiol. A* **159**, 801-811.

Zeil, J., Nalbach, G. and Nalbach, H. O. (1989). Spatial vision in a flat world: optical and neural adaptations in arthropods. In *Neurobiology of Sensory Systems* (ed. R. N. Singh and N. J. Strausfeld), pp. 123-137. New York: Plenum.